

ScholarWorks@GSU

Calculated Vibrational Properties of Asymmetrically Hydrogen Bonded Benzoquinones and Naphthoquinones

Authors	Ilanikashkouli, Mohammadnabi
Citation	Ilanikashkouli, Mohammadnabi. "Calculated Vibrational Properties of Asymmetrically Hydrogen Bonded Benzoquinones and Naphthoquinones." Thesis, Georgia State University, 2021. https://doi.org/10.57709/23980341
DOI	https://doi.org/10.57709/23980341
Download date	2026-03-05 20:31:43
Link to Item	https://hdl.handle.net/20.500.14694/2959

CALCULATED VIBRATIONAL PROPERTIES OF ASYMMETRICALLY HYDROGEN
BONDED BENZOQUINONES AND NAPHTHOQUINONES

by

Mohammad Nabi Ilani Kashkouli

Under the Direction of Samer Gozem, PhD

A Thesis Submitted in Partial Fulfillment of the Requirements for the Degree of

Master of Science

in the College of Arts and Sciences

Georgia State University

2021

ABSTRACT

Quinones are ubiquitous in biochemistry, where they typically function as electron carriers in processes such as photosynthesis and respiration. Quinones bound in protein complexes are often studied using Fourier-transform infrared (FTIR) difference spectroscopy (DS). With FTIR DS it is possible to probe even small changes in hydrogen bonding between the quinones and nearby protein residues. However, the interpretation of FTIR DS is complicated by multiple overlapping contributions to the spectra. Here we employ density functional theory (DFT) based vibrational frequency calculations on benzoquinone (BQ) and naphthoquinone (NQ) model systems to help untangle the intrinsic and environmental factors that could shift the quinone's vibrational mode frequencies and intensities. Specifically, we systematically study the effect that hydrogen bonds and quinone substituents have on the $C = O$ mode vibrational frequencies of the neutral and one-electron reduced BQs and NQs.

INDEX WORDS: DFT, density functional theory; FTIR, Fourier-transform infrared; PQ, plastoquinone; DS, difference spectroscopy; NQ, naphthoquinone; UQ, ubiquinones; ET, electron transfer; PS, photosystem; MQ, menaquinones; PhQ, phylloquinone, FWHM, full-width at half-maximum; 2MNQ, 2-methyl-naphthoquinone; DMNQ, 2,3-dimethyl-naphthoquinone; 2MBQ, 2-methyl-1,4-benzoquinone; EMNQ, 2-ethyl-3-methyl-naphthoquinone

Copyright by
Mohammad Nabi Ilani Kashkouli
2021

CALCULATED VIBRATIONAL PROPERTIES OF ASYMMETRICALLY HYDROGEN
BONDED BENZOQUINONES AND NAPHTHOQUINONES

by

Mohammad Nabi Ilani Kashkouli

Committee Chair: Samer Gozem

Committee: Gary Hasting
Suri S. Iyer

Electronic Version Approved:

Office of Graduate Services
College of Arts and Sciences
Georgia State University
August 2021

DEDICATION

I humbly dedicated this piece of work to my beloved parents, Nasrollah and Aflaltoun, for their endless support, to Katayoun the love of my life, and to my sisters and brother for their inspiring pieces of advice.

ACKNOWLEDGEMENTS

I would like to expressed my deepest appreciation to my advisor, Dr. Samer Gozem for his sincere and selfness support, during my research. I am grateful for his promote and useful advice and the opportunities he has provided me not only in my academic career, but also in my life over last two years. He gives me an unforgettable memory of his benevolence, patience and erudition.

I would also like to thank my thesis committee members, Dr. Gary Hasting and Suri Iyer for their contributions, support and guidance to this work.

I would like to acknowledge the Dr. Gozem lab members, a wonderful group that I have enjoyed working with and learning from them.

TABLE OF CONTENTS

ACKNOWLEDGEMENTS	V
LIST OF TABLES	VIII
LIST OF FIGURES	IX
LIST OF ABBREVIATIONS	XI
1 INTRODUCTION	1
1.1 Photosynthesis	1
1.2 Photosynthetic reaction centers.....	3
1.3 Photosystems I and II.....	4
1.4 Function of quinones in electron transfer pathways.....	5
1.5 Fourier Transform Infrared (FTIR) Spectroscopy	7
1.5.1 Infrared absorbance spectra.....	7
1.5.2 Normal modes.....	10
1.5.3 Difference (DS) and double difference (DDS) FTIR spectroscopy.....	12
1.6 Computational method overview	14
1.7 Thesis overview	16
2 THE EFFECT OF HYDROGEN BONDING ON THE C=O VIBRATIONS OF BENZOQUINONES AND NAPHTHOQUINONES.....	17
2.1 Introduction	17
2.2 Materials and methods	17

2.3	Results and discussion.....	18
2.3.1	<i>The effect of H-bonding on BQ C=O vibrations.....</i>	<i>18</i>
2.3.2	<i>The effect of substituents and H-bonding on the C = O vibrations in naphthoquinones.....</i>	<i>24</i>
3	CONCLUSIONS AND FUTURE WORK.....	30
3.1	Conclusions	30
3.2	Future work	30
3.2.1	<i>Comparison with experimental data.....</i>	<i>31</i>
3.2.2	<i>A more systematic approach to determine intermolecular interaction geometries</i>	<i>31</i>
3.2.3	<i>Local mode analysis method (LMA).....</i>	<i>32</i>
	REFERENCE.....	34

LIST OF TABLES

Table 1 IR spectral regions.....	9
Table 2 Computed $C = O$ vibrational mode frequencies (in cm^{-1}) for the different BQ models. The frequency splitting between the two carbonyl modes is indicated by $\Delta\nu$	24
Table 3 Computed $C=O$ vibrational mode frequencies (in cm^{-1}) for the different NQ models. The frequency splitting between the two carbonyl modes is indicated by $\Delta\nu$	26

LIST OF FIGURES

Figure 1-1 The chloroplast is the photosynthesis factory of the plant. Figure from https://commons.wikimedia.org/wiki/File:Chloroplast_diagram.svg (public domain).....	2
Figure 1-2 The Organization of a thylakoid membrane including four protein complexes. Adapted from http://jonniel.com/en/psIIimages/oxygenicphotosynthmodel.html (Jon Nield, Imperial College, London)	3
Figure 1-3 Structures and schemes of Plastoquinone (PQ) and ubiquinone (UQ).....	6
Figure 1-4 Menaquinones (MQs) are identical to PhQ except in the degree of saturation of the hydrocarbon tail.....	7
Figure 1-5 A sample of IR spectrum for a secondly amine.....	8
Figure 1-6 Different vibrational modes: a) Stretching b) Bending.....	12
Figure 1-7 Optimized structures of the neutral and anionic BQ with H-bonded water molecule: 1n) neutral form 1a) anionic form.	15
Figure 2-1 Optimized geometries and numbering of BQ model H-bonded complexes with water molecules in neutral and anion states. The solid- green line shows the H-binds to carboxyl oxygen. A) Neutral states: (1n) BQ with one water molecule. (2n1) BQ with two water molecules, structure 1. (2n2) BQ with two water molecules, structure 2. (3n1) BQ with three water molecules, structure 1, (3n2) BQ with three water molecules, structure 2. (4n) BQ with four molecules water. B) Anion states: (1a) BQ with one water molecule. (2a1) BQ with two water molecules, structure 1. (2a2) BQ with two water molecules, structure 2. (3n1) BQ with three water molecules, structure 1, (3a2) BQ with three water molecules, structure 2. (4a) BQ with four water molecules.....	19

Figure 2-2 Calculated DS vibrational frequencies for BQ H-bonded to varying numbers of water molecules.	23
Figure 2-3 Optimized geometries of NQ model H-bonded complexes with one water molecule in neutral and anion states. The solid- green line shows the H-binds to carboxyl oxygen A) Neutral states: NQ(n). <i>2MNQ(n1)</i> Methyl-NQ, structure 1. <i>2MNQ(n2)</i> methyl-NQ, structure 2. <i>DMNQ(n)</i> Dimethyl-NQ. <i>EMNQ(n1)</i> Ethyl-methyl-NQ, structure 1. <i>EMNQ(n2)</i> Ethyl-methyl-NQ, structure 2. B) Anion states: (<i>NQ(a)</i>). <i>2MNQ(a1)</i> Methyl-NQ, structure 1. <i>2MNQ(a2)</i> Methyl-NQ, structure 2. <i>DMNQ(a)</i> Dimethyl-NQ. <i>EMNQ(a1)</i> Ethyl-methyl NQ, structure1. <i>EMNQ(a2)</i> Ethyl-methyl NQ, structure 2.	25
Figure 2-4 Calculated Anion minus Neutral DS for the various NQ models H-bonded to one water molecule. Frequencies are unscaled.....	26
Figure 2-5 One water – no water difference spectrum of the neutral species.	27
Figure 2-6 One water – no water difference spectrum of the anionic species.....	28
Figure 3-1 Approach to find potential phyloquinone-water interaction. 1) molecule should be optimized in gas phase 2) place an oxygen atom at each point surround phyloquinone 3) Added two hydrogen atoms to each oxygen to get number of water positions	32

LIST OF ABBREVIATIONS

2MBQ - 2-methyl-1,4-benzoquinone

2MNQ - 2-methyl-1,4-naphthoquinone

AMBER - Assisted model building with energy refinement

ATP - Adenosine triphosphate

B3LYP - Becke, three-parameter, Lee-Yang-Parr exchange-correlation functional

BQ - Benzoquinone

C=O - Carbonyl

DDS - Double difference spectrum

DFT – Density functional theory

DMNQ- 2,3-dimethyl-1,4-naphthoquinone

DS - Difference spectrum

ET- Electron transfer

EMNQ - Ethyl -methyl- naphthoquinone

FTIR - Fourier transform infrared

FWHM- Full width at half maximum

H-bond – Hydrogen band

IR - Infrared spectroscopy

MM - Molecular mechanics

MQ - Menaquinones

NADPH - Nicotinamide adenine dinucleotide phosphate

NMR - Nuclear magnetic resonance

NQ – Naphthoquinone

P 700 - Chlorophyll dimer

PDB - Protein data bank

PhQ - Phylloquinone

PQ - Plastoquinone

PS I- Photosystem I

PS II - Photosystem II

QM - Quantum mechanics

Rb. Sphaeroides- Rhodobacter sphaeroides

RC - Reaction center

UQ - Ubiquinone

1 INTRODUCTION

1.1 Photosynthesis

All living organisms on earth, including humans, require energy to provide the metabolic reactions of development, growth and reproduction. In other words, life on earth depends on photosynthesis, which is a process carried out by plants, algae and different types of bacteria. During photosynthesis, solar energy is converted to chemical energy by absorbing light from the sun with the help of the water and carbon dioxide.[1] The photosynthetic organisms, depending on whether they evolve with oxygen or not, can be categorized into oxygenic and anoxygenic photosynthesis. Oxygenic photosynthesis occurs in plants, algae and bacteria such as cyanobacteria, and allows for carbon fixation. On the other hand, anoxygenic photosynthesis uses light to extract electrons from molecules other than water and does not produce oxygen. Organisms that undergo anoxygenic photosynthesis include green sulfur bacteria, purple bacteria and heliobacteria.[2]

The overall oxygenic photosynthesis process can be divided into two phases[3]: Light-dependent reactions, which occur in the presence of light, and light-independent reactions or dark reaction, which occurs in the absence of light. Light-dependent reactions take place in the thylakoid membranes of the chloroplasts, which are flattened sacs of the membrane. Energy from sunlight is captured in the thylakoid membrane by the pigment chlorophyll. The inner section inside the thylakoid is called lumen, which is the site of the first part of photosynthesis and the space that surrounds the thylakoid is filled with a fluid called stroma where carbon dioxide is used to produce glucose as the second part of photosynthesis[4]. Figure 1.1 shows different parts of chloroplast.

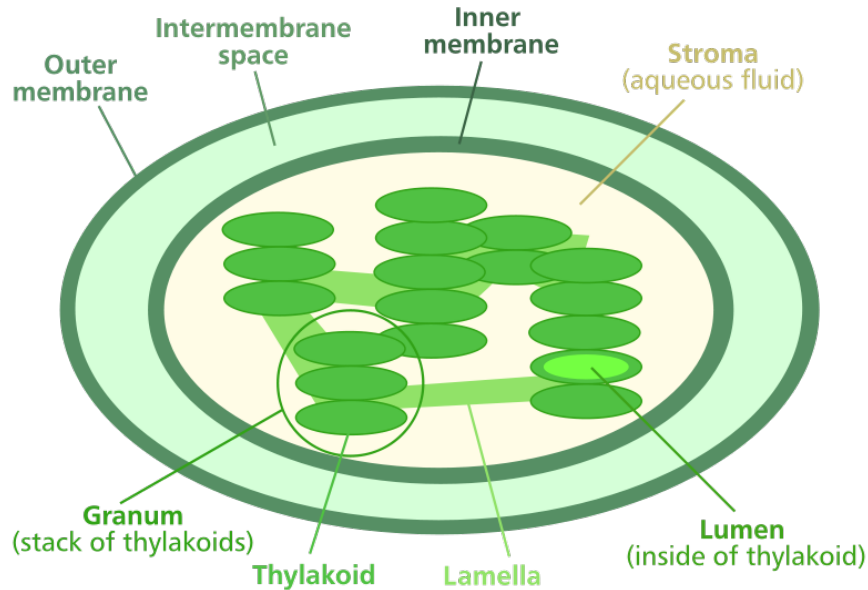


Figure 1-1 The chloroplast is the photosynthesis factory of the plant. Figure from https://commons.wikimedia.org/wiki/File:Chloroplast_diagram.svg (public domain).

Thylakoid membranes play an integral role in light-harvesting and the light-dependent reactions of photosynthesis. The organization of a thylakoid membrane is shown in figure 1.2. The schematic model represents thylakoid membrane components which are involved in light reaction of photosynthesis. There are four protein complexes including photosystem I (PS I), photosystems II (PS II), cytochrome (b_6-f), and ATP synthase. The two photosystems act in series and each has a critical pigment for photosynthesis. Cytochrome is located between two photosystems and catalyze the transfer of electrons of mitochondrial electron transport chain. ATP synthesis take place on the stromal side of the thylakoids where the ATP is required for the light-independent reactions of photosynthesis[4].

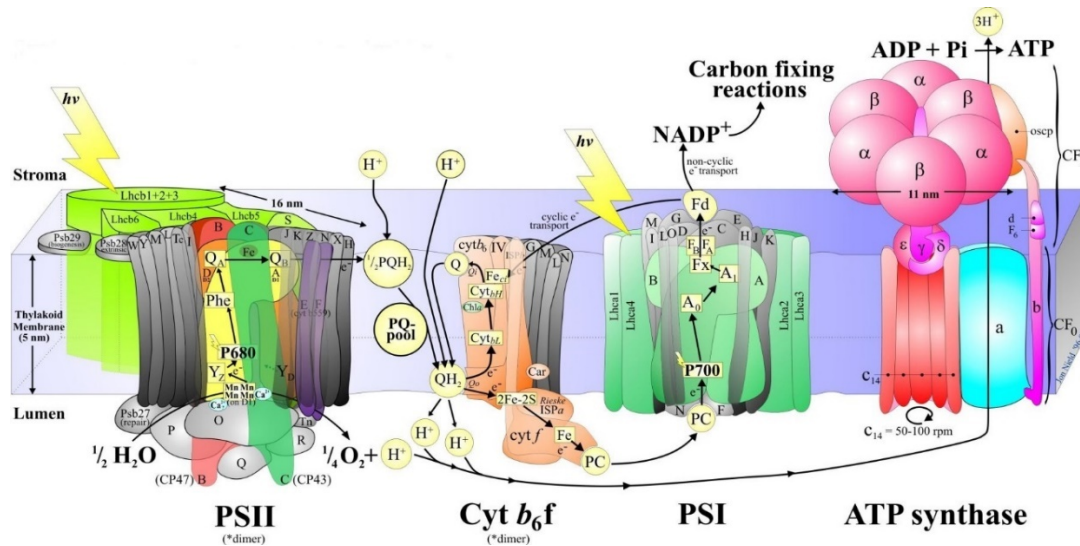


Figure 1-2 The Organization of a thylakoid membrane including four protein complexes. Adapted from <http://jonniel.com/en/psIIimages/oxygenicphotosynthmodel.html> (Jon Nield, Imperial College, London)

In this organization PS I, PS II, and cytochrome work side by side in plants to drive the redox reactions and simultaneously generate a potential gradient across the thylakoid membrane while using light energy and the energy of potential gradient used to generate ATP by ATP synthase. Besides, PS II is responsible for splitting water into protons and oxygen[5].

1.2 Photosynthetic reaction centers

The photosynthetic reaction centers are nature's solar batteries. They can be found in many bacteria, algae and plants and are counted as the heart of biological solar energy conversion. The primary energy conversion reactions of photosynthesis is carried out in photosynthetic reaction center (RC) and this reaction center consists of pigments, proteins and other co-factors such as quinones. In all photosynthetic systems, RCs are responsible for electron transfer and photochemical charge separation. After the initial photon captured by antenna

pigments, an electron is transferred to the RC pigments, which gives rise to a separation and stabilization of charge across the photosynthetic membrane[6, 7].

The photosynthetic reaction centers can be categorized into two different types based on the nature of electron acceptors. While plants, algae, and cyanobacteria have both types of reactions centers, anoxygenic photosynthetic bacteria typically only have one reaction center. Type I reaction centers (RC I) , which can be found in Heliobacteria and green-sulfur bacteria, utilize iron-sulfur [Fe – S] clusters as terminal electron acceptors while type II RCs (RC II) are used by green non-sulfur bacteria, green plant and purple bacteria, and use quinones as a terminal electron acceptor. PS I are associated with type I RCs and PS II are associated with type II RCs[8].

1.3 Photosystems I and II

As discussed earlier, PS I and PS II are functional photosynthetic pigments that are located in thylakoid membrane of chloroplasts and work together to absorb and transfer energy, which implies transfer of electrons. During the light transmission process, PS II takes action first, although it is named PS II because it was discovered after PS I by treatment of lamellar fragments with neutral detergents[9]. Both of the photosystems organization have two main moieties: One moiety is the core complex where the photochemical reactions take place, and the second moiety is the system of antennas that increase the light harvesting potential[10].

PS II is the first link in the chain of the photosynthesis and captures photon from the light to oxidize the two molecules of water to molecular oxygen, releasing four electrons and four hydrogen ions in the process (Figure 1.2). These electrons are passed through electron transport chain. Plastoquinone (PQ) is responsible for carrying electrons from PS II to

cytochrome b_f complex. This photosystem consists of chlorophyll B, chlorophyll A-670, chlorophyll A-680, chlorophyll A-695, chlorophyll A-700, phycobilin, xanthophylls pigments and P680 reaction center. The final stage of the light reaction is catalyzed by PS I which includes chlorophyll B, chlorophyll A-680, chlorophyll A-670, chlorophyll A-695, chlorophyll A-700, and carotenoids and P700 reaction center and also two subunits namely *psaA* and *psaB* which are larger than the subunits of PS II (D_1 and D_2). In this photosystem, the absorbed photons are carried into reaction center (P700) which undergoes a series of electron carriers to supply energy to reduce NADP to NADPH. This process is required for carbon fixation. In PS I, phylloquinone is primarily the cofactor transfers electrons.

Although both PS II and PS I are protein complexes that harvest photons and use light energy in oxygenic photosynthesis, they have differences: The main difference is that PS I pigments absorb longer wavelength of light (> 680 nm), whereas PS II pigments absorb shorter wavelengths of light (< 680 nm). Photosystem I is located at the outer surface of thylakoid membrane and has a photocenter called P700, which is an iron-sulfur (FeS) reaction center. It is not associated with photolysis of water and reducing $NADP^+$ to $NADPH$. On the other hand, PS II is located at inner surface of thylakoid membrane and has a photocenter called P680 which is a quinone-type reaction center. PS II is capable of oxidizing of water and associate with photolysis of water[11].

1.4 Function of quinones in electron transfer pathways

Quinones are a ubiquitous class of compounds found in living organisms, including plants, fungi, and animals.[12] Examples of such naturally occurring quinones are phylloquinone (PhQ, or vitamin K_1), ubiquinone (UQ, or coenzyme Q_{10}), and plastoquinone (PQ), all of which

play integral roles as electron carriers in photosynthesis and respiration in a range of biological systems. PQ is involved in PS II, UQ and menaquinones (MQ) in purple bacteria, and PhQ in PS I. PQs function as terminal ET cofactors in both the Q_A and Q_B binding sites in the reaction center of PS II from oxygen-evolving organisms. UQs play a very similar role in purple non-sulfur bacteria[13]. While identical quinones occupy the Q_A and Q_B binding sites in PSII and purple bacteria, respectively, the functional role of the quinones in these different binding sites is very different. Q_A is an ET component that only undergoes one-electron reduction to form a semiquinone species. On the other hand, Q_B is involved in two-electron reduction and proton uptake to form a hydroquinone species[14]. As shown in figure 1.3, PQ and UQ are made up of an active benzoquinone attached to a side chain and both quinones are substituted benzoquinones (BQ) with an unsaturated hydrophobic tail as ring substituents at adjacent positions between the two C=O groups.

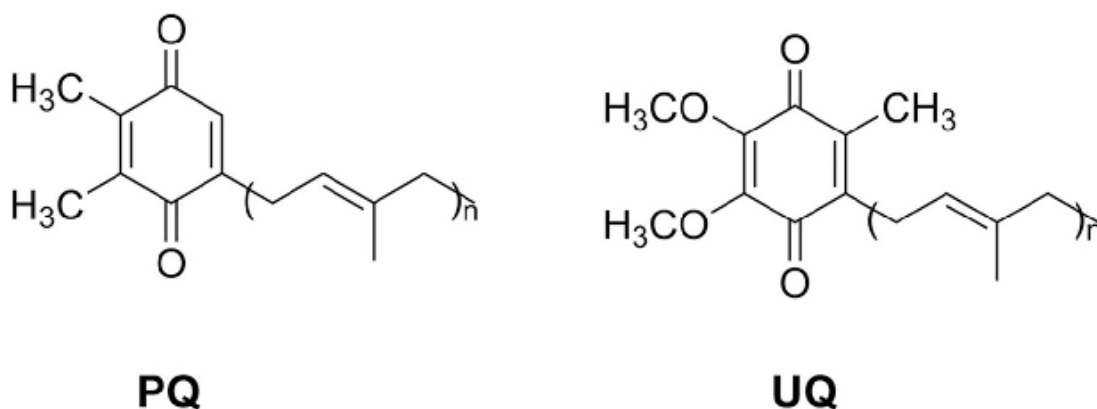


Figure 1-3 Structures and schemes of Plastoquinone (PQ) and ubiquinone (UQ)

The different functional roles of the same quinone in the two binding sites is one example how different protein substituents can modulate the bound quinones' properties.

In the Q_A binding site in purple bacterial reaction centers from *Blastochloris Viridis* and *Chloroflexus Aurantiacus*, MQ (and not UQs) are found in the Q_A binding site[15]. MQs are di-substituted naphthoquinones (NQ) that differ from PhQ only in the degree of saturation of the hydrocarbon attached to the NQ ring[16]. PhQ functions as a low redox potential ET intermediate in PSI RCs[17].

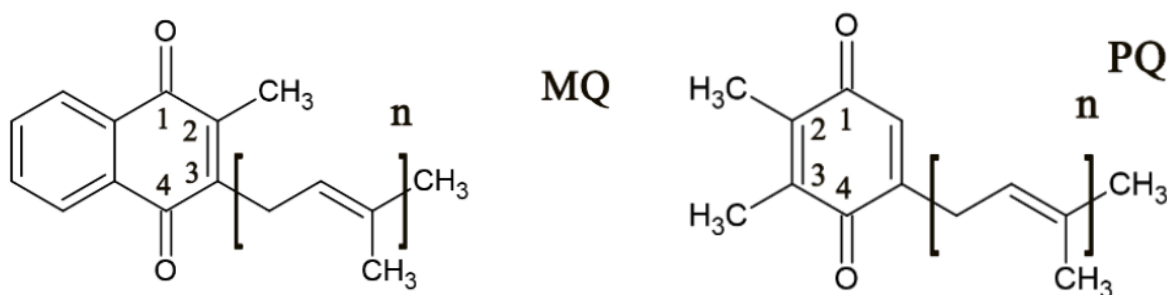


Figure 1-4 Menaquinones (MQs) are identical to PhQ except in the degree of saturation of the hydrocarbon tail

1.5 Fourier Transform Infrared (FTIR) Spectroscopy

1.5.1 Infrared absorbance spectra

Polyatomic molecules have quantized energy levels for each of their rotational, vibrational, electronic, and translational modes. Differences in energy between vibrational energy levels match the energy of electromagnetic radiation in the infrared region of the electromagnetic radiation. For this reason, infrared (IR) spectroscopy is a useful tool for probe and monitor vibrational energy levels in various molecules. IR spectra can reveal important information including bond and angle parameters, hydrogen bonding, and chemical structure of the vibration group which help to characterize a specific molecule. In other words, IR

spectroscopy is a practical tool which can be establish a distinctive signature or figure print for a specific molecular sample.

IR radiation at particular frequencies that are resonant with differences in vibrational energy levels in a molecule are absorbed by molecules and can be plotted in an IR spectrum. In such a plot, the vertical axis shows transmittance or infrared light absorbance and the horizontal axis shows wavenumber (cm^{-1}) (or wavelength). Figure 1.5 shows a sample of IR spectrum for a secondary amine.

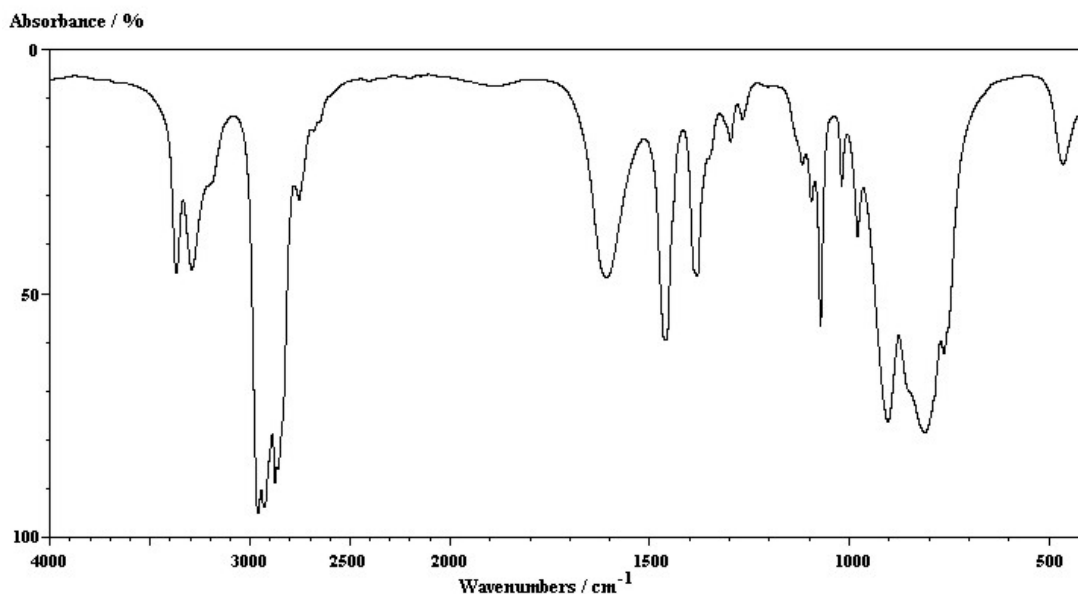


Figure 1-5 A sample of IR spectrum for a secondly amine.

Typically, the IR spectrum is divided into three main spectral regions according to the frequencies of infrared radiation relative to the visible spectrum: Near-infrared, mid-infrared and far infrared. Near-infrared has a wavelength range closest to the red end of the visible light spectrum. The wavelength of near-infrared is between 0.78 to 2.5 microns (0.78-2.5 μm) and has the shortest wavelengths and highest frequencies compared to other IR regions. The mid-infrared

region has a wavelength between 2.5 to 50 microns and used to study fundamental vibrations and related to vibrational-rotational structure. The far-infrared is the farthest region from the frequency of visible light and closest to the microwaves on the electromagnetic spectrum. The wavelength in this region is between 50 to 100 microns and has the longest wavelengths and lowest frequencies. The far region specifically is useful for inorganic studies because of stretching and bending vibration between ligands and metal atoms. Table 1.1 shows various IR spectral regions with their wavelength and wavenumbers[18].

Table 1 IR spectral regions

Region	Wavelength(μm)	Wavenumbers (V), cm^{-1}	Frequencies (ν), HZ
Near	0.78-2.5	12800 - 4000	3.8×10^{14} - 1.2×10^{14}
Middle	2.5-50	4000 - 200	3.8×10^{14} - 1.2×10^{14}
Far	50-100	200 -10	3.8×10^{14} - 1.2×10^{14}
Most Used	2.5-15	4000 -670	3.8×10^{14} - 1.2×10^{14}

IR Spectroscopy, compared to other techniques, provides some benefits in studies of biological systems. In the first place, IR spectra can provide structural information such as about the presence of functional groups of a compound. In some cases, especially when combined with theoretical calculations, IR spectra can also provide information about the position of the substituent group, and the structure and stereochemistry of the compound. Thus, IR spectroscopy has become a useful tool to identify and detect various kinds of compounds.

In addition to the ability of IR spectroscopy to probe structural information of a compound, there are other strengths to consider as well. The sample phase for analysis in principle does not have many constraints and may be liquid, gas or solid, which has expanded the range of analytes more

than some other spectroscopies that are usually constrained to one or two phases. IR spectroscopy can also be used to study both large complexes and small molecules. Finally, IR can also probe intermolecular interactions such as van der Waals forces, hydrogen bonding, and intermolecular interactions. However, while IR spectra give useful information of compounds, it has also some limitations. IR spectra cannot predict the mass of a substance nor easily give information about the position of functional groups[19].

1.5.2 Normal modes

In a molecule, all atoms are in a motion regularly. There are three types of motions for molecules: translations which are external motions, rotations and vibrations which are internal motions. Normal modes are used to explain various vibrational motions in molecules. In each normal mode, all atoms of a certain molecule are vibrating in phase and have same frequency. For normal modes, each vibration does not depend on other vibration and various molecule vibrate at different frequencies and have different normal modes[20].

It is easy to calculate the number of normal modes for a molecule which has N atoms. $3N$ is the total number of coordinates to describe the position of molecule in three-dimensional space (3D-space). $3N$ is referred to total number of degrees of freedom of a molecule, given by the fact that each of the N atoms of the molecule has three degrees of freedom in 3D space. Of those $3N$ total degrees of freedom, three correspond to translational degrees of freedom and two (linear molecule) or three (non-linear) correspond to rotational degrees of freedom. Nonlinear molecules therefore have $3N - 6$ normal modes of vibration, while linear molecules have $3N - 5$ normal modes of vibration. To illustrate the point, CO_2 has three atoms ($N = 3$) and is a linear molecule. As a result, it has $3N = 9$ total degrees of freedom. It consists of 3 translational, 2

rotational degrees of freedom, and 4 vibrational degrees of freedom, since it is a linear molecule[21].

In complex or polyatomic molecules there are more than one bonds and various types of vibrations can occur. These vibrations can be generally be classified into two main categories: stretching and bending.

In stretching vibrations, the bond lengths in the molecule that are related by symmetry vibrate, either by symmetric stretching or asymmetric stretching. A symmetric stretch happens when atoms move in phase (lengthening or shortening at the same time). As a consequence, when the bonds are located across from each other, symmetric stretching leads to no change in the dipole moment. On the other hand, in asymmetric vibrations, the length of one bond is decreases as the other one increases, and therefore some atoms move out of phase with respect to others. Asymmetric stretches are usually accompanied by changes in the dipole moment, and therefore are IR-active.

In bending stretching, a change occurs between angles of the molecule while the bond lengths remain unchanged. Atoms can bend in four different ways: scissoring, rocking (which take place within the plane of the molecule) wagging and twisting (which take place outside of the plane of molecule). Vibrational modes are shown in figure 1.6.

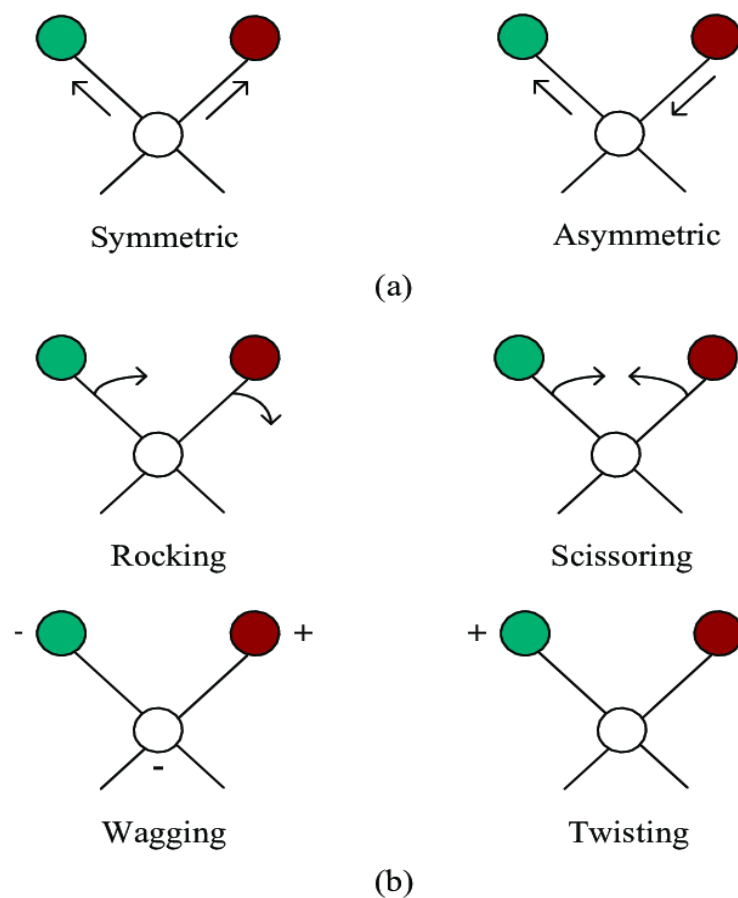


Figure 1-6 Different vibrational modes: a) Stretching b) Bending

1.5.3 Difference (DS) and double difference (DDS) FTIR spectroscopy

The Fourier transfer method was proposed in IR spectroscopy as an alternative to the more traditional IR spectroscopy (using monochromatic light with varying wavenumbers). FTIR uses broadband light with different frequencies to retrieve the IR spectrum through a Fourier transform. In comparison with traditional IR spectroscopy, FTIR has a higher signal to noise, higher speed, and provides more accurate wavenumber measurements.

In large biological systems, IR spectra becomes more complex and it is hard to determine which peaks are related to which groups since the many different bands overlap. These overlapping bands in absorption spectra place a limit on information that can be obtained from IR spectroscopy of these systems. In this regard, difference spectroscopy (DS) is a valuable method to solve this problem. Bands can be highlighted by subtracting one absorption spectrum from another, particularly in a case where a protein undergoes some change, such as an electronic reduction. For instance, reduced – oxidized DS can provide spectra of both the radical anion and neutral state of the reduced moiety [22]. In this example, negative bands relate to the neutral molecule and positive bands relate to charged molecule.

FTIR DS has been widely applied to probe quinones' interaction with neighboring groups in various photosynthetic proteins[23-26]. FTIR DS is exquisitely sensitive to small changes in hydrogen-bonding to the carbonyl groups of bound quinones[27]. Such FTIR DS have been experimentally measured for the reduction of quinones from the neutral oxidized state to both the reduced quinone and semiquinone states[28, 29]. FTIR DS thus is a powerful method to probe the protein micro-environment surrounding flavin and measure the effect of reduction in a single spectrum.

The interpretation of FTIR DS can be complicated by various effects that can shift the IR spectral band peaks. The frequencies of quinones' vibrational modes are usually shifted by their interaction with the nearby protein environment by effects such as hydrogen bonding and coupling with other vibrational modes of the protein. In the past, some FTIR DS experiments have been aided by quantum chemical calculations computations that model the IR spectra of the quinones in solution and proteins. Examples of such calculations include density functional

theory (DFT) vibrational frequencies for quinones in solution[30-33] as well as hybrid quantum mechanical/molecular mechanical (QM/MM) calculations or cluster models that explicitly treat the protein-pigment interactions of different quinone binding sites[34-36].

1.6 Computational method overview

Computational chemistry can be implemented to vibrational spectroscopy for a better characterization of all bands of the spectra and can simulate different phases of compound to interpret their spectra[37]. Basically, computational chemistry implements theoretical chemistry incorporated into efficient computer programs to calculate structure and properties of molecules such as vibrational frequencies, relative energies, dipole moments and charge distributions.

Density functional theory (DFT) is one the most powerful technique to study electronic structure of molecules. DFT methods evolved from the theorems of Hohenberg and Kohn[38]. Those theorems declare that the electron density and electronic Hamiltonian have a functional relationship, which enables the computation of all ground-state molecular properties without a wave function. This means that it is feasible to predict properties of molecule subsequent to determination of three coordinates, no matter what is the size of the molecule[39, 40]. Using DFT, it is possible to predict many properties of molecules such as energies, structures and vibrational frequencies [41].

In the calculations reported in this thesis, the quinones such as BQs and NQs are treated at the quantum mechanical level using density functional theory (DFT) based method. Calculations were carried out using Gaussian16. The Gaussian 16 calculation requires an initial structure in the input file, typically provided in Cartesian coordinates. This structure can be built in one of various available graphical user interfaces such as Gaussview[42] or IQmol.[43]. The

geometry of structure is then optimized. The geometry optimizations and frequency calculations in the neutral and one-electron reduced states were performed with the B3LYP [44] functional and the 6-31+G(d) basis set. Figure 1.6 shows optimized structures of the neutral (oxidized) and anionic (one-electron reduced semiquinone) BQ with H-bonded water molecule in a gas phase. The neutral and anionic states are differentiated in the inputs due to their different multiplicities and charges. Note that, as a result of these differences, the position of water near $C_1 = O$ for the two states are not in a similar position due.

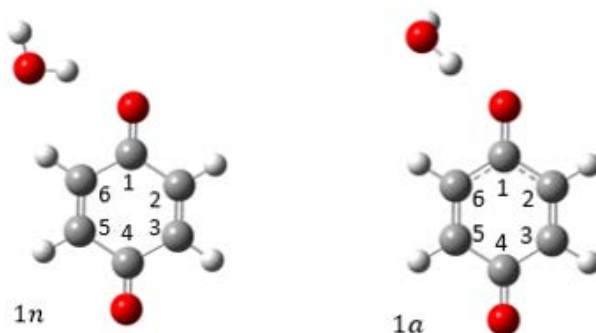


Figure 1-7 Optimized structures of the neutral and anionic BQ with H-bonded water molecule: 1n) neutral form 1a) anionic form.

1.7 Thesis overview

This dissertation aims to provide computations that can be used as a reference to study the structural properties of quinones in the RCs by using benzoquinone (BQ) and naphthoquinone (NQ) model systems. The current chapter has introduced the background information on the photosynthetic RCs. The function of quinones in electron transfer pathways was discussed and FTIR difference spectroscopy is described as a tool to understand shift of frequencies of quinones their interaction with the nearby protein environment by effects such as hydrogen bonding and coupling with other vibrational modes of the protein.

In chapter 2, BQs and NQs optimized structures in both neutral and one electron reduced states are shown by the B3LYP functional and the 6-31+G(d) basis set. To understand the effect of hydrogen bonding on C=O vibration for BQ, six neutral and six anionic structures were obtained with a varying number of H-bonded water molecules and different arrangement. C=O vibrational frequencies (in wavenumbers) of different modeled BQ were computed. Furthermore, the effect of the water position on C=O vibrations in presence of substituent (Methyl group) is discussed. Geometries were obtained for model H-bonded complexes with one water molecule in neutral and anion states for NQs with different substituent including Methyl-NQ, Dimethyl-NQ, Ethyl-methyl-NQ to understand the effect of substituents and hydrogen bonding on the C=O vibrations in naphthoquinones. DS were plotted by subtracting the FTIR spectra of structures without water from that with water to get a better understanding of the effect of adding a water molecule in these structures.

2 THE EFFECT OF HYDROGEN BONDING ON THE C=O VIBRATIONS OF BENZOQUINONES AND NAPHTHOQUINONES

2.1 Introduction

Benzoquinones (BQs) and naphthoquinones (NQs) play critical role in biological proton and electron transfer processes in photosynthesis and respiration [46]. This study employs simple unsubstituted BQs and NQs as model systems to disentangle intrinsic and environmental effects that shift the C=O vibrational frequencies. Specifically, we systematically study the impact of single H bonds, multiple H bonds, the position of the H bond, and substituent effects on the C=O vibrations of BQs and NQs. Existing studies have focused on the structure and vibrational frequencies of the bio-relevant quinones such as plastoquinone and phylloquinone to a large extent. However, using such models that are already H-bonded and substituted makes it challenging to disentangle the factors that decouple and shift the C=O vibrational frequencies. The driving force for this work is to focus on small model systems with minimal substituents, to better disentangle the various effects that affect C=O vibrational frequencies.

2.2 Materials and methods

BQ and NQ geometry optimizations and frequency calculations in the neutral and one-electron reduced states were performed using the B3LYP functional and the 6-31+G(d) basis set. Water molecules (ranging from one to four water molecules) were manually added to the gas phase structures at different positions such that they are H-bonded with the quinone carbonyl groups. The structures were then re-optimized in the presence of those water molecules without atomic constraints. The computed IR stick spectra were broadening using Gaussian functions with a 4 cm⁻¹ full-width at half-maximum (FWHM). Simulated difference spectra were generated by subtracting one broadened computed FTIR spectrum from another using the Origin Lab

software. All quantum mechanical calculations were performed with the Gaussian16 program package. Gauss View 6 was used to visualize the structures and animations of the vibrational modes.

2.3 Results and discussion

2.3.1 *The effect of H-bonding on BQ C=O vibrations*

Six neutral and six anionic structures were obtained to investigate the effect of H-bonding on BQ $C=O$ vibrations. Figure 2.1 shows optimized structures of the neutral (oxidized) and anionic (one-electron reduced semiquinone) BQ with a varying number of H-bonded water molecules. The naming convention (e.g., $2n_1$) indicates the number of water molecules used as the prefix, whether the molecule is in the neutral or anionic redox state (n is used for neutral, a for anionic), and, in some cases, the arrangement of the water molecules as a subscript (e.g., $2n_1$ indicates one optimized structure distinct from $2n_2$).

One pair of neutral/anionic structures includes only one water H-bonded to the $C_1=O$ ($1n$ and $1a$). Two pairs of structures were obtained with two water molecules; one pair of structures has only one water molecule H-bonded to the $C_1=O$ carbonyl and the other water H-bonded to the water ($2n_1$ and $2a_1$), while another pair of structures had both water molecules directly H-bonded to the $C_1=O$ carbonyl ($2n_2$ and $2a_2$). Attempts to optimize three water molecules bonded to a single carbonyl in the neutral state were unsuccessful, as expected, and we instead optimized a structure with one H-bonded water directly H-bonded to the $C_1=O$ carbonyl and forming an H-bonding network with the other two water molecules ($3n_1$). Meanwhile, a structure with three water molecules directly interacting with the $C_1=O$ carbonyl was successfully optimized for the anionic state ($3a_1$). We also optimized a second structure with two water molecules H-bonded at $C_1=O$ and a third water molecule H-bonded at $C_4=O$ ($3n_2$ and $3a_2$). Finally, for both the

neutral and anionic states, we optimized a structure with two water molecules H-bonded to $C_1 = O$ and two water molecules H-bonded to $C_4 = O$ ($4n$ and $4a$).

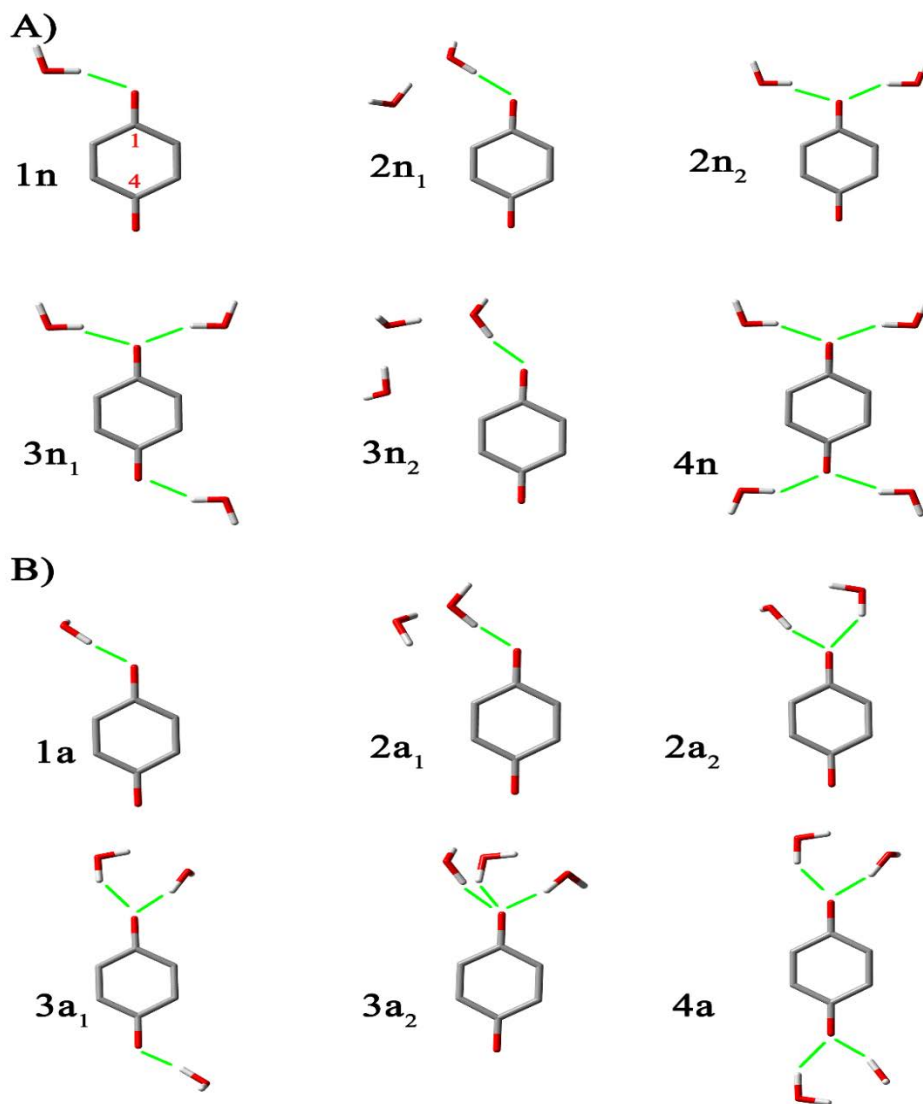


Figure 2-10 Optimized geometries and numbering of BQ model H-bonded complexes with water molecules in neutral and anion states. The solid- green line shows the H-binds to carboxyl oxygen. A) Neutral states: ($1n$) BQ with one water molecule. ($2n_1$) BQ with two water molecules, structure 1. ($2n_2$) BQ with two water molecules, structure 2. ($3n_1$) BQ with three water molecules, structure 1, ($3n_2$) BQ with three water molecules, structure 2. ($4n$) BQ with four molecules water. B) Anion states: ($1a$) BQ with one water molecule. ($2a_1$) BQ with two water molecules, structure 1. ($2a_2$) BQ with two water molecules, structure 2. ($3a_1$) BQ with three water molecules, structure 1, ($3a_2$) BQ with three water molecules, structure 2. ($4a$) BQ with four water molecules

Fig. 2.2 shows the computed anion-neutral DS for these optimized structures for neutral and anion states in the $1800 - 1400 \text{ cm}^{-1}$ spectral region. Positive peaks in the DS spectra are FTIR peaks corresponding to the anionic state, while negative peaks correspond to the neutral state. Our discussion will focus on the $C = O$ vibrational peaks since these are often the most prominent in the experimental DS spectra. Because the H-bonding structures of various quinones are reflected in the IR spectra, these calculations can help provide an interpretation of experimental spectra to determine H-bonding structures.

In the neutral states, the $C = O$ peaks appear in the $1750\text{-}1650 \text{ cm}^{-1}$ spectral region, in the left-most boxed part in Fig. 2.2 The $\nu(C_1 = O)$ and $\nu(C_4 = O)$ peaks were identified by visual inspection of the vibrational modes in GaussView. The corresponding wavenumbers and splitting between those two peaks ($\Delta\nu$) are tabulated in Table 2. In organic solvents and in proteins, neutral quinone $C = O$ bands are expected in $1700\text{-}1600 \text{ cm}^{-1}$ range, while semiquinone CO bands are expected in the $1550\text{-}1400 \text{ cm}^{-1}$. The computed wavenumbers are therefore upshifted with respect to the experiments, as expected by the fact that B3LYP/6-31G* computed frequencies often need to be scaled by a constant smaller than 1.

Neutral BQ that is free from H-bonding displays an antisymmetric and symmetric coupled C=O vibration at 1736 cm^{-1} and 1738 cm^{-1} , respectively. The anti-symmetric vibration carries nearly all the intensity, with the symmetric vibration being nearly IR silent. For neutral BQ with the $C_1=O$ group H-bonded to one water molecule (1n model in Fig. 2.1), the C=O modes are very weakly coupled. The calculated frequency of the $C_1 = O$ mode is found at 1726 cm^{-1} , 10 cm^{-1} lower in frequency than that of the non-H-bonded BQ. The $C_4 = O$ mode frequency remains unchanged although the intensities of the modes is altered (Table 2).

Adding a second water molecule near the $C_1 = O$ carbonyl group causes a very large downshift in the $\nu(C_1 = O)$ mode frequency to 1661-1674 cm^{-1} . Interestingly, this large downshift is observed for both types of BQ H-bonded models with two water molecules ($2n_2$, $\nu(C_1 = O) = 1661\text{ cm}^{-1}$, $2n_1$, $\nu(C_1 = O) = 1674\text{ cm}^{-1}$). For the $2n_1$ and $2n_2$ BQ molecular models, the $\nu(C_4 = O)$ mode frequency is essentially unaltered compared to the 1n model.

For the $3n_1$ and $3n_2$ molecular models, the placement of the water molecules has a large influence on the frequency shifts. When all three water molecules are on the same side of the molecule ($3n_2$), with one of the water molecules hydrogen bonded to the $C_1 = O$ mode, the $\nu(C_1 = O)$ vibrational mode is strongly downshifted relative to the model with no hydrogen bonds, and therefore the $\Delta\nu$ between $\nu(C_1 = O)$ and $\nu(C_4 = O)$ is large (73 cm^{-1}). On the other hand, when one of the water molecules is on the opposite side and hydrogen bonded to $C_4 = O$, $\Delta\nu$ is reduced considerably to 25 cm^{-1} .

The $4n$ structure has each of its $C = O$ groups involved in two H-bonds. For this model, the $C = O$ vibrational modes are again coupled as symmetric and asymmetric vibrational modes as in BQ. The modes are also partly coupled with water bending motions. $\Delta\nu$ in $4n$ is reduced further to 22 cm^{-1} compared to other hydrogen bonded models, but does not become as small as in the BQ structure with no hydrogen bonds. Therefore, even when both carbonyl groups are equally H-bonded, $\nu_{sym}(C = O)$ and $\nu_{asym}(C = O)$ are not equally affected by this H-bonding; the $\nu_{asym}(C = O)$ is more sensitive to hydrogen bonding (more downshifted) than the $\nu_{sym}(C = O)$.

In the BQ anion, the $C = O$ mode frequencies are downshifted $\sim 200 - 250\text{ cm}^{-1}$ relative to neutral BQ (see Fig. 2.1 and the associated Table 2). For experimental anion minus

neutral FTIR DS, this large difference is very useful as the neutral and anion modes do not overlap, simplifying interpretation.

Visual inspection of the vibrational modes of all the BQ anion (BQ⁻) models reveals that the $C = O$ modes are symmetrically and antisymmetrically coupled and are separated by 50 – 60 cm^{-1} (Table 2). For all BQ⁻ models (whether H-bonded or not) a weak $\nu_{sym}(C = O)$ mode is calculated near 1485 cm^{-1} and an intense $\nu_{asym}(C = O)$ mode is calculated near 1544 cm^{-1} . The calculations with a varying number of water molecules clearly shows that the $C = O$ modes of BQ⁻ are not sensitive to H-bonding, and the splitting between the two modes ($\Delta\nu$) remains relatively constant at 55 – 59 cm^{-1} . The relative intensities of the symmetric and asymmetric C=O modes are sensitive to H-bonding, however (Table 2).

The obtained data here is fully consistent with results by Ashikawa et al. for plastoquinone. Specifically, they similarly found that $C = O$ vibrational frequencies in neutral plastoquinone become downshifted by hydrogen bonding, but that the intense $\nu_{asym}(C = O)$ band frequency is not sensitive to the hydrogen bonding interactions.

Overall, DFT calculations on BQ with a different number of water molecules indicate that the $C = O$ stretching frequencies are sensitive to the number of H-bonds in the neutral state. Specifically, while adding one water has a small downshifting effect (5 – 12 cm^{-1}), adding two water molecules on the same carbonyl group has a larger (more than additive) downshifting effect (21 – 65 cm^{-1}). This finding is consistent with calculations by Bandaranayake et al., who previously demonstrated splitting of $C = O$ bands by asymmetric H-bonding interactions with plastoquinone in the neutral state. On the other hand, calculations for BQ⁻ show a minimal effect of H-bonding on the stretching frequencies of the carbonyl peaks. This is consistent with a joint

computational and experimental study that shows that $C = O$ stretching modes of reduced plastoquinone are not sensitive to the number and asymmetry of H-bonding agents.[45] The effect of unequal H-bonding on $C_1 = O$ and $C_4 = O$ is instead limited to an increase of the intensity of the $\nu_{sym}(C = O)$ symmetric stretching peak.

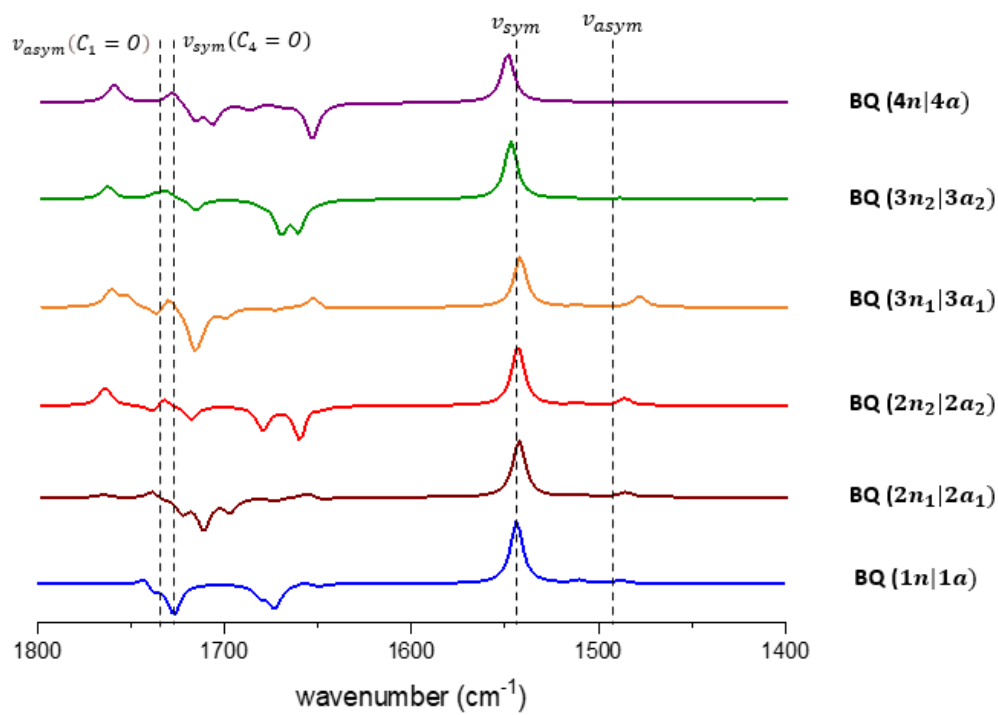


Figure 2-2 Calculated DS vibrational frequencies for BQ H-bonded to varying numbers of water molecules.

Table 2 Computed $C = O$ vibrational mode frequencies (in cm^{-1}) for the different BQ models. The frequency splitting between the two carbonyl modes is indicated by $\Delta\nu$.

H-bonding structure	Neutral forms					Anion forms				
	$\nu(C_1 = O)$ or asymmetric (cm^{-1})	IR intensity	$\nu(C_4 = O)$ or symmetric (cm^{-1})	IR intensity	$(\Delta\nu)$ (cm^{-1})	ν_{sym} (cm^{-1})	IR Intensity	ν_{asym} (cm^{-1})	IR Intensity	$(\Delta\nu)$ (cm^{-1})
BQ	1736	449	1738	0.2	2	1492	0.02	1542	478	50
BQ ($1n 1a$)	1726	282	1738	92	12	1488	28	1543	569	55
BQ ($2n_1 2a_1$)	1674	33	1738	102	64	1487	49	1544	578	57
BQ- ($2n_2 2a_2$)	1661	397	1739	101	78	1487	75	1544	633	57
BQ ($3n_1 3a_1$)	1714	159	1739	110	25	1485	129	1543	598	58
BQ ($3n_2 3a_2$)	1661	446	1734	23	73	1489	13	1548	860	59
BQ ($4n 4a$)	1711	89	1733	0.0	22	1491	0.1	1550	1027	59

2.3.2 The effect of substituents and H-bonding on the $C = O$ vibrations in naphthoquinones

Fig. 2.3 shows optimized geometries of NQ with different sidechain substituents at the 2 or 3 positions, in the presence of one water molecule, for both neutral and anion states. For NQs that lack C_{2v} symmetry (i.e., 2MNQ and EMNQ), two structures were considered with a water molecule placed either near the $C_1 = O$ ($2n_1$ and $4a_1$) or the $C_4 = O$ ($2n_2$ and $4a_2$) (Fig. 2.3).

Fig. 2.4 shows the calculated anion minus neutral FTIR DS in the $1800 - 1400 \text{ cm}^{-1}$ region for the various models in Fig. 2.4. Positive/negative peaks in the DS correspond to the anion/neutral state, respectively. For neutral state quinones, $C = O$ peaks are found in the ~ 1750 - 1700 cm^{-1} region. The $\nu(C_1 = O)$ and $\nu(C_4 = O)$ peaks were identified by the visual inspection of animations of the vibrational modes. In the NQ anion, the $C = O$ mode frequencies are downshifted by $\sim 180 - 220 \text{ cm}^{-1}$ relative to neutral state (in the 1550 - 1450 cm^{-1} spectral region). Similar to the anionic BQ, the $\nu_{sym}(C = O)$ have virtually no intensity, while the $\nu_{asym}(C = O)$ modes are relatively intense. The calculated frequencies of the ($C = O$) modes and their frequency difference ($\Delta\nu$) are listed in Table 3.

Since all the plots in Fig. 2.3 are for molecules hydrogen bonded to a single water, differences in FTIR DS can be attributed to the substituents. The results show that alkyl substituents invariably downshift the $C = O$ vibrational frequencies relative to NQ in both the neutral and the anionic systems, with larger substituents having a larger effect.

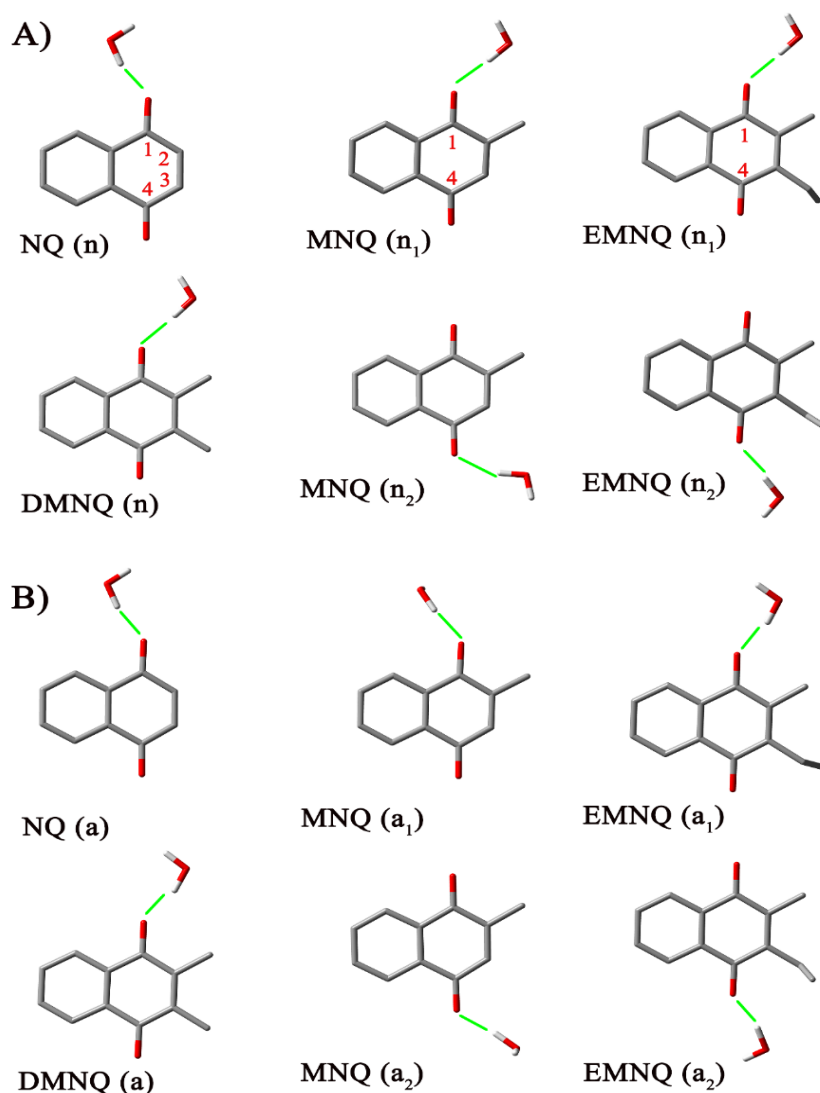


Figure 2-3 Optimized geometries of NQ model H-bonded complexes with one water molecule in neutral and anion states. The solid- green line shows the H-binds to carboxyl oxygen
 A) Neutral states: NQ(n). 2MNQ(n_1) Methyl-NQ, structure 1. 2MNQ(n_2) methyl-NQ, structure 2. DMNQ(n) Dimethyl-NQ. EMNQ(n_1) Ethyl-methyl-NQ, structure 1. EMNQ(n_2) Ethyl-methyl-NQ, structure 2. B) Anion states: (NQ(a). 2MNQ(a_1) Methyl-NQ, structure 1. 2MNQ(a_2) Methyl-NQ, structure 2. DMNQ(a) Dimethyl-NQ. EMNQ(a_1) Ethyl-methyl NQ, structure 1. EMNQ(a_2) Ethyl-methyl NQ, structure 2.

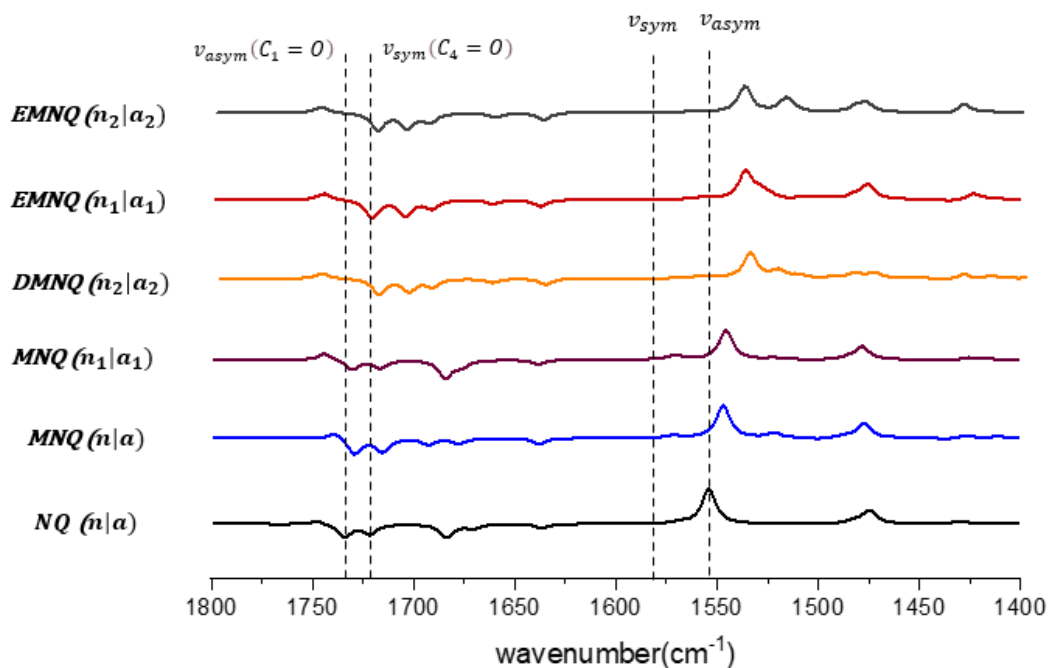


Figure 2-4 Calculated Anion minus Neutral DS for the various NQ models H-bonded to one water molecule. Frequencies are unscaled.

Table 3 Computed C=O vibrational mode frequencies (in cm-1) for the different NQ models. The frequency splitting between the two carbonyl modes is indicated by $\Delta\nu$.

H-bonding structure	Neutral forms					Anion forms				
	$\nu(C_1 = O)$ or asymmetric (cm^{-1})	IR intensity	$\nu(C_4 = O)$ or symmetric (cm^{-1})	IR intensity	$(\Delta\nu)$ (cm^{-1})	ν_{sym} (cm^{-1})	IR Intensity	ν_{asym} (cm^{-1})	IR Intensity	$(\Delta\nu)$ (cm^{-1})
NQ	1721	159	1734	211	13	1501	7	1554	556	53
MNQ ($n a$)	1715	200	1729	241	14	1521	72	1547	488	23
MNQ ($n_1 a_1$)	1716	130	1730	158	14	1521	26	1545	473	24
DMNQ ($n_2 a_2$)	1705	187	1720	227	15	1522	11	1536	374	14
EMNQ ($n_1 a_1$)	1704	198	1721	225	17	1523	12	1536	354	13
EMNQ ($n_2 a_2$)	1705	194	1719	217	14	1517	144	1538	330	19

For neutral NQ, 2-methyl-naphthoquinone (2MNQ), 2,3-dimethyl-naphthoquinone (DMNQ), and 2-ethyl-3-methyl-naphthoquinone (EMNQ) the C=O modes are coupled, giving rise to a weak/intense $\nu_{sym}(C=O)/\nu_{asym}(C=O)$ vibrations in the 1750-1700 cm^{-1} region.

To better visualize how the C=O normal modes are impacted by hydrogen bonding, or the effect of adding a H-bonded water molecule to the structure, we plot in Figs. 2.5 and 6 DS obtained by subtracting the FTIR spectra of structures without water (structures not shown) from that with one water (structures in Fig. 2.3). While this is not an experimentally obtainable FTIR DS (at least, not easily obtainable), this theoretical exercise helps highlight the effect of hydrogen bonding on the vibrational modes.

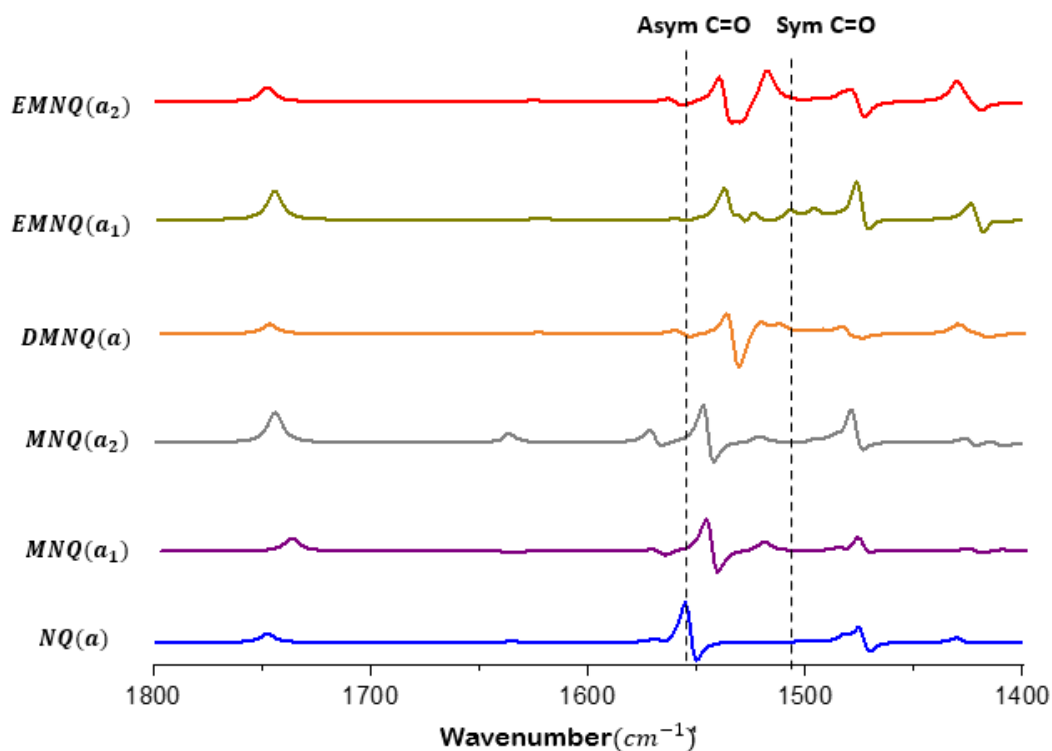


Figure 2-5 One water – no water difference spectrum of the neutral species.

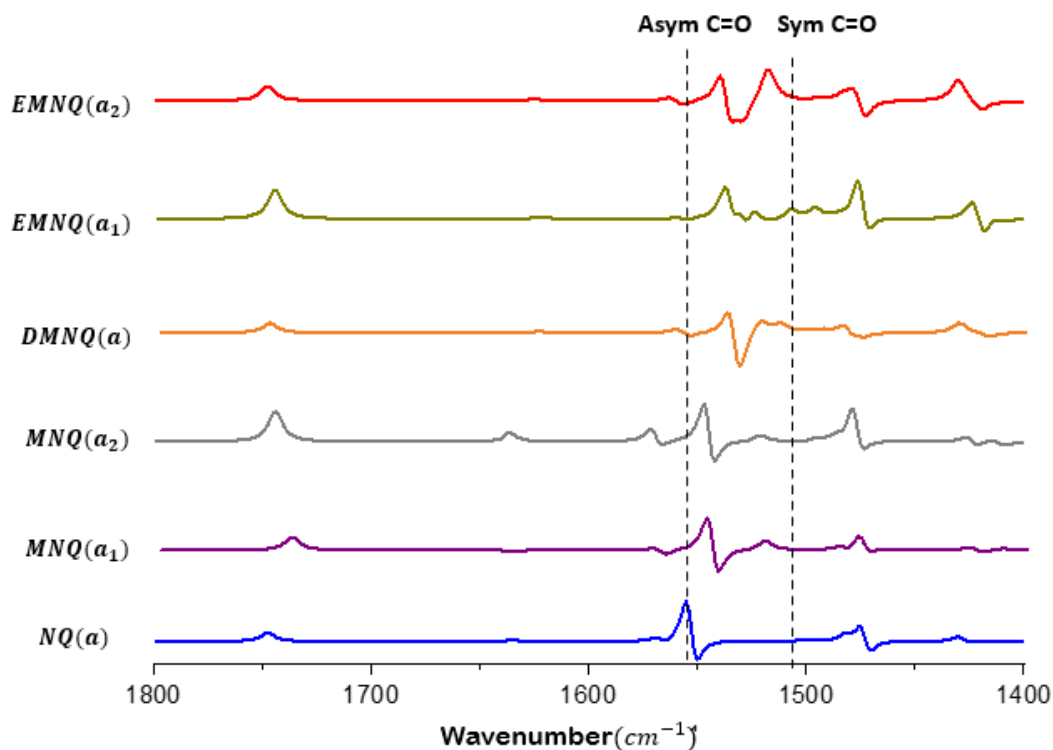


Figure 2-6 One water – no water difference spectrum of the anionic species.

The neutral NQ “water – no water DS” (Fig. 2.5) clearly shows that the addition of a water molecule to each structure downshifts the $\nu_{asym}(C=O)$ mode vibrations. This trend is consistent for all substituted NQs. On the other hand, the $\nu_{sym}(C=O)$ mode vibrations do not appear to be affected by the hydrogen bonding, although it is affected by the substituents.

Fig. 2.6 shows the “water – no water DS” for the anionic states of the various substituted NQs. Not much can be said here about the effect of hydrogen bonding on the $\nu_{sym}(C=O)$ mode vibrational frequency, since this peak has no intensity. However, the $\nu_{asym}(C=O)$ mode vibrations are clearly upshifted by hydrogen bonding relative to the spectrum with no water. This

is the opposite trend than that observed in the neutral NQs, where hydrogen bonding downshifts the $\nu_{asym}(C=O)$ mode vibrations.

3 CONCLUSIONS AND FUTURE WORK

3.1 Conclusions

Quinones function as electron carriers in processes such as photosynthesis and respiration. FTIR DS is a technique to probe their interactions in protein complexes. With FTIR DS it is possible to probe even small changes in hydrogen bonding between the quinones and nearby protein residues.

DFT calculations were performed using the B3LYP functional in combination with the 6-31+G(d) basis set to demonstrate that simple quinones such as naphthoquinones and benzoquinones are useful as model systems for studying intrinsic and environmental effects on C=O vibrations. We use these models to study the effect of H-bonding interactions on C=O stretching vibrations and attempt to disentangle the various effects such as the number of H-bonds with each carbonyl group, the position of the H-bonding water molecules, and the effect of alkyl substituents on the vibrational frequencies of the C=O group.

For symmetric neutral quinones (e.g., BQ, NQ, and DMNQ), H-bonding splits the degeneracy of the two C=O peaks. The extent of splitting is dependent on the number of H-bonding interactions at each carbonyl. Calculations on the anionic states of benzoquinones show that the prominent C=O vibrations are not very sensitive to H-bonding; only their relative intensities are noticeably affected since the symmetric stretch gains some intensity when there is a different number of H-bonding interactions at each C=O.

3.2 Future work

This thesis presents study of vibrational properties quinones in photosynthetic reaction centers (RCs) using FTIR DS in combination with density functional theory (DFT) calculations.

FTIR DS is a useful tool for probing the substituents of quinones in protein binding sites to advance the research on the structural feature studies in terms of vibrational bands. In this section, some potential improvements to the model and to this work are presented:

3.2.1 Comparison with experimental data

This work focuses on a purely hypothetical computational experiment, where water molecules are placed at specific positions around a quinone to determine the effect of that hydrogen-bonding interaction on the FTIR spectrum of the neutral and anionic states. However, such an experiment cannot be performed (at least, not easily) in practice. An important step forward for this work is to connect the calculations with experimental data. This could be by comparison with related experimental data in the literature (e.g., comparison of FTIR spectra in solvents with varying degree of hydrogen bonding), or by collaboration with new experiments.

3.2.2 A more systematic approach to determine intermolecular interaction geometries

The approach in this work involves manual placement of water molecules near the quinones and optimizing to find a local minimum structure. The result may, to an extent, depend on the initial geometry prepared manually. To avoid this, a more systematic approach is needed. In the future, an approach similar to Kabir et al[46], based on “electrostatic tuning maps” [47] can be used to study hydrogen bonding interactions in a more systematic way and including more potential quinone–water interaction geometries.

In this thesis, we tried to add a limit number of hydrogen bonding near the carbonyl group to find potential water interactions. To find such potential interactions, we can optimize the different quinones such as PQ, PhQ, UQ and MQ in gas phase. After the optimization. We

place an oxygen atom at various points on a surface that is some multiple of a van der Waals radius of the molecule. Two hydrogen atoms are then added to each oxygen to obtain a uniform water positions surrounding the main molecule. Finally, in the presence of each one of these waters, we run the individual geometry optimization and frequency calculation for the quinone–water pair.

Figure 3.1 illustrates with approach for finding potential phyloquinone–water interactions. This approach can be applied for both neutral and anion forms

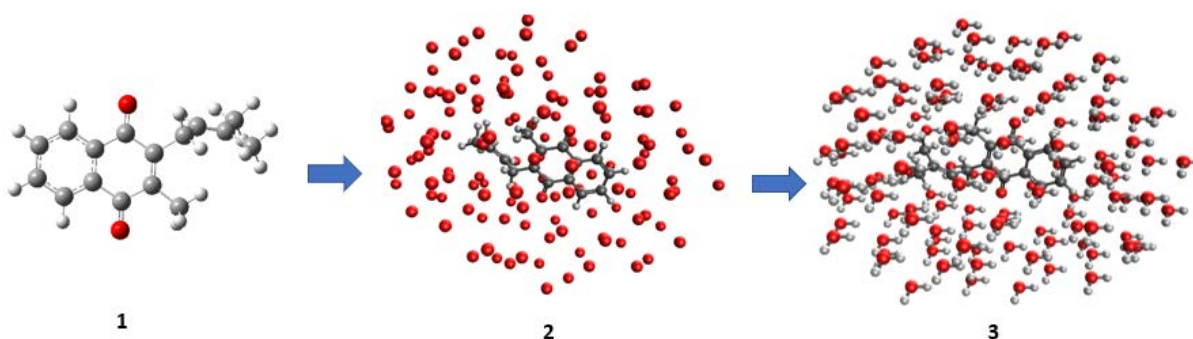


Figure 3-1 Approach to find potential phyloquinone-water interaction. 1) molecule should be optimized in gas phase 2) place an oxygen atom at each point surround phyloquinone 3) Added two hydrogen atoms to each oxygen to get number of water positions

3.2.3 Local mode analysis method (LMA)

Local mode analysis method [48] can be a powerful tool to study the effect of hydrogen bonding on purely localized C=O vibrations and to further analyze the direct effect of hydrogen bonding on the electronic character of the C=O bond vs. the effect of coupling with water bending vibrational modes. The method characterizes the motions of atoms of the corresponding IR bands and provides direct access to the structural information encoded in IR spectra. A normal

mode decomposition into local modes [49] could also be used to check how hydrogen bonding affects the contributions of local modes to the C=O dominant normal modes.

REFERENCE

1. Blankenship, R.E. and H. Hartman, *The origin and evolution of oxygenic photosynthesis*. Trends in biochemical sciences, 1998. **23**(3): p. 94-97.
2. Hunter, C.N., et al., *The purple phototrophic bacteria*. Vol. 28. 2008: Springer Science & Business Media.
3. Fromme, P., P. Jordan, and N. Krauß, *Structure of photosystem I*. Biochimica et Biophysica Acta (BBA)-Bioenergetics, 2001. **1507**(1-3): p. 5-31.
4. Arnon, D.I., *The Light Reactions of Photosynthesis*. Proceedings of the National Academy of Sciences, 1971. **68**(11): p. 2883-2892.
5. Nelson, N. and C.F. Yocum, *STRUCTURE AND FUNCTION OF PHOTOSYSTEMS I AND II*. Annual Review of Plant Biology, 2006. **57**(1): p. 521-565.
6. Deisenhofer, J. and J.R. Norris, *Photosynthetic Reaction Center*. Vol. 2. 2013: Academic Press.
7. Olson, J.M., *Evolution of photosynthetic reaction centers*. Biosystems, 1981. **14**(1): p. 89-94.
8. Blankenship, R.E., *Origin and early evolution of photosynthesis*. Photosynthesis research, 1992. **33**(2): p. 91-111.
9. Rogers, K., *The chemical reactions of life: from metabolism to photosynthesis*. 2010: Britannica Educational Publishing.
10. Horton, P., A. Ruban, and R. Walters, *Regulation of light harvesting in green plants*. Annual review of plant biology, 1996. **47**(1): p. 655-684.
11. Caffarri, S., et al., *A comparison between plant photosystem I and photosystem II architecture and functioning*. Current Protein and Peptide Science, 2014. **15**(4): p. 296-331.
12. Abraham, I., et al., *Recent advances in 1, 4-benzoquinone chemistry*. Journal of the Brazilian Chemical Society, 2011. **22**(3): p. 385-421.
13. de Wijn, R. and H.J. Van Gorkom, *Kinetics of electron transfer from QA to QB in photosystem II*. Biochemistry, 2001. **40**(39): p. 11912-11922.
14. D Lambrev, M., et al., *Structure/function/dynamics of photosystem II plastoquinone binding sites*. Current Protein and Peptide Science, 2014. **15**(4): p. 285-295.
15. Zhu, Z. and M. Gunner, *Energetics of quinone-dependent electron and proton transfers in Rhodospirillum rubrum photosynthetic reaction centers*. Biochemistry, 2005. **44**(1): p. 82-96.
16. Beulens, J.W., et al., *The role of menaquinones (vitamin K2) in human health*. British Journal of Nutrition, 2013. **110**(8): p. 1357-1368.
17. Rappaport, F. and B.A. Diner, *Primary photochemistry and energetics leading to the oxidation of the (Mn) 4Ca cluster and to the evolution of molecular oxygen in Photosystem II*. Coordination Chemistry Reviews, 2008. **252**(3-4): p. 259-272.
18. Zeitler, J., et al., *Nondestructive quantification of pharmaceutical tablet coatings using terahertz pulsed imaging and optical coherence tomography*. Journal of Pharmacy and Pharmacology, 2007. **59**: p. 209-223.
19. Smith, B.C., *Fundamentals of Fourier transform infrared spectroscopy*. 2011: CRC press.

20. Twardowski, J., P. Anzenbacher, and M.R. Masson, *Raman and IR spectroscopy in biology and biochemistry*. 1994: Ellis Horwood.
21. Harris, D.C. and M.D. Bertolucci, *Symmetry and spectroscopy: an introduction to vibrational and electronic spectroscopy*. 1989: Courier Corporation.
22. Breton, J., et al., *Probing the primary quinone environment in photosynthetic bacterial reaction centers by light-induced FTIR difference spectroscopy*. FEBS letters, 1991. **278**(2): p. 257-260.
23. Breton, J., et al., *Binding sites of quinones in photosynthetic bacterial reaction centers investigated by light-induced FTIR difference spectroscopy: assignment of the interactions of each carbonyl of QA in Rhodobacter sphaeroides using site-specific ¹³C-labeled ubiquinone*. Biochemistry, 1994. **33**(48): p. 14378-14386.
24. Noguchi, T., *Fourier transform infrared difference and time-resolved infrared detection of the electron and proton transfer dynamics in photosynthetic water oxidation*. Biochimica et Biophysica Acta (BBA)-Bioenergetics, 2015. **1847**(1): p. 35-45.
25. Thibodeau, D., et al., *Time-resolved FTIR spectroscopy of quinones in Rb. sphaeroides reaction centers*. Biochimica et Biophysica Acta (BBA)-Bioenergetics, 1990. **1020**(3): p. 253-259.
26. Suzuki, H., et al., *Fourier transform infrared spectrum of the secondary quinone electron acceptor QB in photosystem II*. Biochemistry, 2005. **44**(34): p. 11323-11328.
27. Breton, J. and E. Navedryk, *Protein-quinone interactions in the bacterial photosynthetic reaction center: light-induced FTIR difference spectroscopy of the quinone vibrations*. Biochimica et Biophysica Acta (BBA)-Bioenergetics, 1996. **1275**(1-2): p. 84-90.
28. Hastings, G., *Vibrational spectroscopy of photosystem I*. Biochimica et Biophysica Acta (BBA)-Bioenergetics, 2015. **1847**(1): p. 55-68.
29. Makita, H. and G. Hastings, *Time-resolved step-scan FTIR difference spectroscopy for the study of photosystem I with different benzoquinones incorporated into the A1 binding site*. Biochimica et Biophysica Acta (BBA)-Bioenergetics, 2018. **1859**(11): p. 1199-1206.
30. Zhan, C.-G. and D.M. Chipman, *Effect of Hydrogen Bonding on the Vibrations of p-Benzosemiquinone Radical Anion*. The Journal of Physical Chemistry A, 1998. **102**(7): p. 1230-1235.
31. Nonella, M., G. Mathias, and P. Tavan, *Infrared spectrum of p-benzoquinone in water obtained from a QM/MM hybrid molecular dynamics simulation*. The Journal of Physical Chemistry A, 2003. **107**(41): p. 8638-8647.
32. Agarwala, N., et al., *Calculated and Experimental Infrared Spectra of Substituted Naphthoquinones*.
33. Yadav, R., N. Singh, and R. Yadav, *Vibrational studies of trifluoromethyl benzene derivatives: II 5-amino-2-fluoro and 5-amino-2-chloro benzotrifluorides*. Indian Journal of Physics, 2003. **77**: p. 421-427.
34. Rohani, L. and G. Hastings, *Vibrational Properties of Quinones in the A1 Binding Site of Photosystem I Calculated Using a Three-Layer ONIOM Method*.
35. Rohani, L., et al., *Calculated vibrational properties of semiquinones in the A1 binding site in photosystem I*. Biochimica et Biophysica Acta (BBA)-Bioenergetics, 2019. **1860**(9): p. 699-707.
36. Lamichhane, H.P. and G. Hastings, *Calculated vibrational properties of pigments in protein binding sites*. Proceedings of the National Academy of Sciences, 2011. **108**(26): p. 10526-10531.

37. Palafox, M.A., *Computational chemistry applied to vibrational spectroscopy: A tool for characterization of nucleic acid bases and some of their 5-substituted derivatives*. Physical Sciences Reviews, 2017. **2**(8).
38. Kohn, W., A.D. Becke, and R.G. Parr, *Density functional theory of electronic structure*. The Journal of Physical Chemistry, 1996. **100**(31): p. 12974-12980.
39. Alex, A.A., *4.16 - Quantum Mechanical Calculations in Medicinal Chemistry: Relevant Method or a Quantum Leap Too Far?*, in *Comprehensive Medicinal Chemistry II*, J.B. Taylor and D.J. Triggle, Editors. 2007, Elsevier: Oxford. p. 379-420.
40. Dobson, J.F., G. Vignale, and M.P. Das, *Electronic density functional theory: recent progress and new directions*. 2013.
41. Frisch, M., et al., *Gaussian 16*. 2016, Gaussian, Inc. Wallingford, CT.
42. Frisch, A., A. Nielson, and A. Holder, *Gaussview user manual*. Gaussian Inc., Pittsburgh, PA, 2000. **556**.
43. Gilbert, A., *IQmol molecular viewer*. 2012.
44. Lee, C., W. Yang, and R.G. Parr, *Development of the Colle-Salvetti correlation-energy formula into a functional of the electron density*. Physical review B, 1988. **37**(2): p. 785.
45. Agarwala, N., et al., *Calculated and Experimental Infrared Spectra of Substituted Naphthoquinones*. Front. Sci. Technol. Eng. Math., 2019. **3**(2).
46. Kabir, M.P., et al., *The Effect of Hydrogen-Bonding on Flavin's Infrared Absorption Spectrum*. Spectrochimica Acta Part A: Molecular and Biomolecular Spectroscopy, 2021: p. 120110.
47. Orozco-Gonzalez, Y., M.P. Kabir, and S. Gozem, *Electrostatic spectral tuning maps for biological chromophores*. The Journal of Physical Chemistry B, 2019. **123**(23): p. 4813-4824.
48. Kraka, E., W. Zou, and Y. Tao, *Decoding chemical information from vibrational spectroscopy data: Local vibrational mode theory*. Wiley Interdisciplinary Reviews: Computational Molecular Science, 2020. **10**(5): p. e1480.
49. Konkoli, Z. and D. Cremer, *A new way of analyzing vibrational spectra. III. Characterization of normal vibrational modes in terms of internal vibrational modes*. International journal of quantum chemistry, 1998. **67**(1): p. 29-40.
1. Blankenship, R.E. and H. Hartman, *The origin and evolution of oxygenic photosynthesis*. Trends in biochemical sciences, 1998. **23**(3): p. 94-97.
2. Hunter, C.N., et al., *The purple phototrophic bacteria*. Vol. 28. 2008: Springer Science & Business Media.
3. Fromme, P., P. Jordan, and N. Krauß, *Structure of photosystem I*. Biochimica et Biophysica Acta (BBA)-Bioenergetics, 2001. **1507**(1-3): p. 5-31.
4. Arnon, D.I., *The Light Reactions of Photosynthesis*. Proceedings of the National Academy of Sciences, 1971. **68**(11): p. 2883-2892.
5. Nelson, N. and C.F. Yocum, *STRUCTURE AND FUNCTION OF PHOTOSYSTEMS I AND II*. Annual Review of Plant Biology, 2006. **57**(1): p. 521-565.
6. Deisenhofer, J. and J.R. Norris, *Photosynthetic Reaction Center*. Vol. 2. 2013: Academic Press.
7. Olson, J.M., *Evolution of photosynthetic reaction centers*. Biosystems, 1981. **14**(1): p. 89-94.
8. Blankenship, R.E., *Origin and early evolution of photosynthesis*. Photosynthesis research, 1992. **33**(2): p. 91-111.

9. Rogers, K., *The chemical reactions of life: from metabolism to photosynthesis*. 2010: Britannica Educational Publishing.
10. Horton, P., A. Ruban, and R. Walters, *Regulation of light harvesting in green plants*. Annual review of plant biology, 1996. **47**(1): p. 655-684.
11. Caffarri, S., et al., *A comparison between plant photosystem I and photosystem II architecture and functioning*. Current Protein and Peptide Science, 2014. **15**(4): p. 296-331.
12. Abraham, I., et al., *Recent advances in 1, 4-benzoquinone chemistry*. Journal of the Brazilian Chemical Society, 2011. **22**(3): p. 385-421.
13. de Wijn, R. and H.J. Van Gorkom, *Kinetics of electron transfer from QA to QB in photosystem II*. Biochemistry, 2001. **40**(39): p. 11912-11922.
14. D Lambreva, M., et al., *Structure/function/dynamics of photosystem II plastoquinone binding sites*. Current Protein and Peptide Science, 2014. **15**(4): p. 285-295.
15. Zhu, Z. and M. Gunner, *Energetics of quinone-dependent electron and proton transfers in Rhodospirillum rubrum photosynthetic reaction centers*. Biochemistry, 2005. **44**(1): p. 82-96.
16. Beulens, J.W., et al., *The role of menaquinones (vitamin K2) in human health*. British Journal of Nutrition, 2013. **110**(8): p. 1357-1368.
17. Rappaport, F. and B.A. Diner, *Primary photochemistry and energetics leading to the oxidation of the (Mn) 4Ca cluster and to the evolution of molecular oxygen in Photosystem II*. Coordination Chemistry Reviews, 2008. **252**(3-4): p. 259-272.
18. Zeitler, J., et al., *Nondestructive quantification of pharmaceutical tablet coatings using terahertz pulsed imaging and optical coherence tomography*. Journal of Pharmacy and Pharmacology, 2007. **59**: p. 209-223.
19. Smith, B.C., *Fundamentals of Fourier transform infrared spectroscopy*. 2011: CRC press.
20. Twardowski, J., P. Anzenbacher, and M.R. Masson, *Raman and IR spectroscopy in biology and biochemistry*. 1994: Ellis Horwood.
21. Harris, D.C. and M.D. Bertolucci, *Symmetry and spectroscopy: an introduction to vibrational and electronic spectroscopy*. 1989: Courier Corporation.
22. Breton, J., et al., *Probing the primary quinone environment in photosynthetic bacterial reaction centers by light-induced FTIR difference spectroscopy*. FEBS letters, 1991. **278**(2): p. 257-260.
23. Breton, J., et al., *Binding sites of quinones in photosynthetic bacterial reaction centers investigated by light-induced FTIR difference spectroscopy: assignment of the interactions of each carbonyl of QA in Rhodospirillum rubrum using site-specific 13C-labeled ubiquinone*. Biochemistry, 1994. **33**(48): p. 14378-14386.
24. Noguchi, T., *Fourier transform infrared difference and time-resolved infrared detection of the electron and proton transfer dynamics in photosynthetic water oxidation*. Biochimica et Biophysica Acta (BBA)-Bioenergetics, 2015. **1847**(1): p. 35-45.
25. Thibodeau, D., et al., *Time-resolved FTIR spectroscopy of quinones in Rb. sphaeroides reaction centers*. Biochimica et Biophysica Acta (BBA)-Bioenergetics, 1990. **1020**(3): p. 253-259.
26. Suzuki, H., et al., *Fourier transform infrared spectrum of the secondary quinone electron acceptor QB in photosystem II*. Biochemistry, 2005. **44**(34): p. 11323-11328.

27. Breton, J. and E. Nabedryk, *Protein-quinone interactions in the bacterial photosynthetic reaction center: light-induced FTIR difference spectroscopy of the quinone vibrations*. Biochimica et Biophysica Acta (BBA)-Bioenergetics, 1996. **1275**(1-2): p. 84-90.
28. Hastings, G., *Vibrational spectroscopy of photosystem I*. Biochimica et Biophysica Acta (BBA)-Bioenergetics, 2015. **1847**(1): p. 55-68.
29. Makita, H. and G. Hastings, *Time-resolved step-scan FTIR difference spectroscopy for the study of photosystem I with different benzoquinones incorporated into the A1 binding site*. Biochimica et Biophysica Acta (BBA)-Bioenergetics, 2018. **1859**(11): p. 1199-1206.
30. Zhan, C.-G. and D.M. Chipman, *Effect of Hydrogen Bonding on the Vibrations of p-Benzosemiquinone Radical Anion*. The Journal of Physical Chemistry A, 1998. **102**(7): p. 1230-1235.
31. Nonella, M., G. Mathias, and P. Tavan, *Infrared spectrum of p-benzoquinone in water obtained from a QM/MM hybrid molecular dynamics simulation*. The Journal of Physical Chemistry A, 2003. **107**(41): p. 8638-8647.
32. Agarwala, N., et al., *Calculated and Experimental Infrared Spectra of Substituted Naphthoquinones*.
33. Yadav, R., N. Singh, and R. Yadav, *Vibrational studies of trifluoromethyl benzene derivatives: II 5-amino-2-fluoro and 5-amino-2-chloro benzotrifluorides*. Indian Journal of Physics, 2003. **77**: p. 421-427.
34. Rohani, L. and G. Hastings, *Vibrational Properties of Quinones in the A1 Binding Site of Photosystem I Calculated Using a Three-Layer ONIOM Method*.
35. Rohani, L., et al., *Calculated vibrational properties of semiquinones in the A1 binding site in photosystem I*. Biochimica et Biophysica Acta (BBA)-Bioenergetics, 2019. **1860**(9): p. 699-707.
36. Lamichhane, H.P. and G. Hastings, *Calculated vibrational properties of pigments in protein binding sites*. Proceedings of the National Academy of Sciences, 2011. **108**(26): p. 10526-10531.
37. Palafox, M.A., *Computational chemistry applied to vibrational spectroscopy: A tool for characterization of nucleic acid bases and some of their 5-substituted derivatives*. Physical Sciences Reviews, 2017. **2**(8).
38. Kohn, W., A.D. Becke, and R.G. Parr, *Density functional theory of electronic structure*. The Journal of Physical Chemistry, 1996. **100**(31): p. 12974-12980.
39. Alex, A.A., *4.16 - Quantum Mechanical Calculations in Medicinal Chemistry: Relevant Method or a Quantum Leap Too Far?*, in *Comprehensive Medicinal Chemistry II*, J.B. Taylor and D.J. Triggle, Editors. 2007, Elsevier: Oxford. p. 379-420.
40. Dobson, J.F., G. Vignale, and M.P. Das, *Electronic density functional theory: recent progress and new directions*. 2013.
41. Frisch, M., et al., *Gaussian 16*. 2016, Gaussian, Inc. Wallingford, CT.
42. Frisch, A., A. Nielson, and A. Holder, *Gaussview user manual*. Gaussian Inc., Pittsburgh, PA, 2000. **556**.
43. Gilbert, A., *IQmol molecular viewer*. 2012.
44. Lee, C., W. Yang, and R.G. Parr, *Development of the Colle-Salvetti correlation-energy formula into a functional of the electron density*. Physical review B, 1988. **37**(2): p. 785.
45. Agarwala, N., et al., *Calculated and Experimental Infrared Spectra of Substituted Naphthoquinones*. Front. Sci. Technol. Eng. Math., 2019. **3**(2).

46. Kabir, M.P., et al., *The Effect of Hydrogen-Bonding on Flavin's Infrared Absorption Spectrum*. Spectrochimica Acta Part A: Molecular and Biomolecular Spectroscopy, 2021: p. 120110.
47. Orozco-Gonzalez, Y., M.P. Kabir, and S. Gozem, *Electrostatic spectral tuning maps for biological chromophores*. The Journal of Physical Chemistry B, 2019. **123**(23): p. 4813-4824.
48. Kraka, E., W. Zou, and Y. Tao, *Decoding chemical information from vibrational spectroscopy data: Local vibrational mode theory*. Wiley Interdisciplinary Reviews: Computational Molecular Science, 2020. **10**(5): p. e1480.
49. Konkoli, Z. and D. Cremer, *A new way of analyzing vibrational spectra. III. Characterization of normal vibrational modes in terms of internal vibrational modes*. International journal of quantum chemistry, 1998. **67**(1): p. 29-40.